ACS APPLIED MATERIALS & INTERFACES

Letter

www.acsami.org

Polymer/Polymer Blend Solar Cells Improved by Using High-Molecular-Weight Fluorene-Based Copolymer as Electron Acceptor

Daisuke Mori,[†] Hiroaki Benten,*[,†] Hideo Ohkita,[†,‡] Shinzaburo Ito,*[,†] and Kunihito Miyake[§]

[†]Department of Polymer Chemistry, Graduate School of Engineering, Kyoto University, Katsura, Nishikyo, Kyoto 615-8510, Japan

[‡]Japan Science and Technology Agency (JST), PRESTO, 4-1-8 Honcho Kawaguchi, Saitama 332-0012, Japan

[§]Tsukuba Research Laboratory, Sumitomo Chemical Co., Ltd., 6 Kitahara, Tsukuba 300-3294, Japan

Supporting Information

ABSTRACT: The highest power conversion efficiency (PCE) of 2.7% has been achieved for all-polymer solar cells made with a blend of poly(3-hexylthiophene) (P3HT, electron donor) and poly[2,7-(9,9-didodecylfluorene)-*alt*-5,5-(4′,7′-bis(2-thienyl)-2′,1′,3′-benzothiadiazole)] (PF12TBT, electron acceptor). The PCE of the P3HT/PF12TBT solar cells increases from 1.9% to 2.7% with an increase in the molecular weight (M_w) of PF12TBT from 8500 to 78 000 g mol^{-1}. In a device with high-molecular-weight PF12TBT, efficient charge generation is maintained even at high annealing temperatures because of the small phase separation on the length scale of exciton diffusion due to an increase in the glass transition temperature (T_g) and a reduced diffusional mobility of the PF12TBT chains above T_g. On the other hand, efficient charge transport is also achieved through the formation of interconnected networks of PF12TBT-rich domains, which is facilitated by the high molecular weight of PF12TBT, and the ordering of P3HT chains in P3HT-rich domains, which is a result of high-temperature annealing. Thus, when high-molecular-weight PF12TBT is used, an optimal blend morphology that supports efficient charge generation as well as charge transport can be obtained by thermal annealing, and consequently, the highest PCE reported so far for an all-polymer solar cell is achieved.

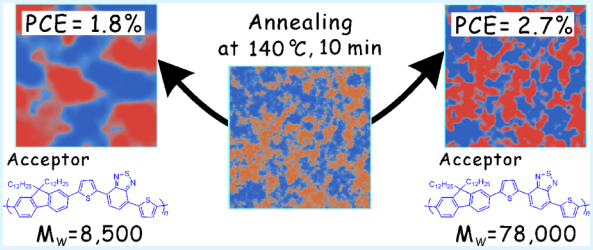

KEYWORDS: *polymer photovoltaics, conjugated polymer blends, phase separation, nanoscale morphology, poly(3-hexylthiophene), fluorene-based copolymer*

To develop all-polymer solar cells with a power conversion efficiency (PCE) comparable to that of polymer/fullerene solar cells,[1−4] it is necessary to understand and control the blend nanomorphology, and considerable efforts have been made to this end.[5−11] However, the PCEs of most all-polymer solar cells are still lower than 2.0%[11−13] because of the blend having undesirable morphological characteristics, such as large phase separation,[14] inhomogeneous internal phase composition,[15−19] and poor crystallinity.[20] Although there are several reports on the control of the phase-separated structures of polymer/polymer blends through the use of cosolvents[13,21,22] and through thermal annealing of the as-spun films,[10,11] it is still a challenge to obtain an optimal blend morphology that supports both efficient charge generation and charge transport at the same time.

In this research, we fabricate polymer/polymer solar cells by blending poly(3-hexylthiophene) (P3HT, Figure 1), which is an electron donor, with poly[2,7-(9,9-didodecylfluorene)-*alt*-5,5-(4′,7′-bis(2-thienyl)-2′,1′,3′-benzothiadiazole)] (PF12TBT, Figure 1), which is as an electron acceptor. The rate of phase separation during thermal annealing is strongly dependent on the molecular weight of PF12TBT, and a maximum PCE of 2.7% is achieved for the device based on high-molecular-weight PF12TBT, as shown in Figure 1. Therefore, we conclude that molecular weight is a key factor that should be considered for improving the PCE of polymer/polymer solar cells.

P3HT/PF12TBT solar cells were fabricated by using PF12TBT with three different molecular weights; the weight-average molecular weights (M_w) are listed in Table 1. The best performance of each device is shown in Table 2. With an increase in M_w, the PCE improved from 1.9% (M_w = 8500 g mol^{-1}) to 2.0% (M_w = 20 000 g mol^{-1}) and 2.7% (M_w = 78 000 g mol^{-1}), which is the highest value reported so far for an all-polymer solar cell. Thus, it is clear that M_w has a significant impact on the solar cell efficiency. As evident from Table 2, the improvement in the PCE can be mainly ascribed to an increase in the fill factor (FF) since both short-circuit current density (J_{SC}) and open-circuit voltage (V_{OC}) were almost identical irrespective of M_w. Furthermore, the optimal annealing temperature increased from 100 °C to 140 °C with an increase in M_w, suggesting that the rate of evolution of the blend morphology during annealing varied with M_w. The difference in the blend morphology is confirmed by atomic force microscopy (AFM) images of the blend films before and after thermal

Received: April 10, 2012
Accepted: June 24, 2012
Published: June 25, 2012

   dx.doi.org/10.1021/am300623f | *ACS Appl. Mater. Interfaces* 2012, 4, 3325−3329

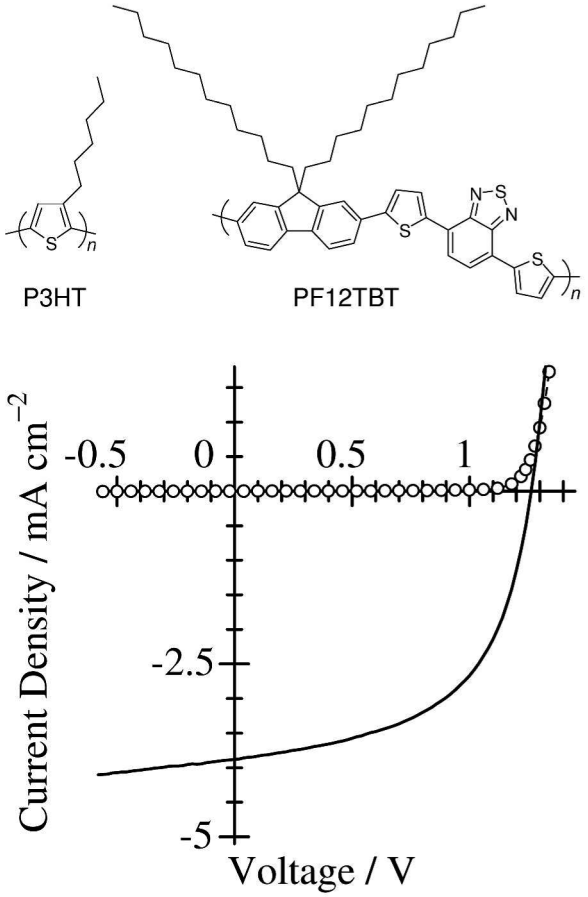

Figure 1. Chemical structures of P3HT and PF12TBT and *J*–*V* characteristics of a P3HT/PF12TBT solar cell with 2.7% PCE under AM 1.5G illumination from a calibrated solar simulator with an intensity of 100 mW cm^{-2} (solid line) and the dark condition (open circles). The molecular weight of PF12TBT was M_w = 78 000 g mol^{-1}. The device was fabricated by spin-coating from a chloroform solution of P3HT and PF12TBT (1:1 weight ratio) and annealed at 140 °C for 10 min. The device parameters are listed in Table 2.

Table 1. Weight-Average Molecular Weight M_w, Number-Average Molecular Weight M_n, Polydispersity Index (PDI), and Glass Transition Temperature (T_g) of PF12TBT Acceptor Polymers Used in This Study

acceptor polymer	M_w (g mol^{-1})	M_n (g mol^{-1})	PDI	T_g (°C)
L–PF12TBT	8500	4900	1.7	60
M–PF12TBT	20 000	10 200	2.0	76
H–PF12TBT	78 000	28 000	2.8	90

annealing at 140 °C for 10 min. For the P3HT/*L*-PF12TBT, as shown in panels a and b in Figure 2, surface roughness was increased from 4 nm to larger than 8 nm and coarsening of the morphology was observed after annealing. For the P3HT/*H*-PF12TBT, as shown in panels c and d in Figure 2, no distinct change in the surface morphology was observed before and after annealing. The different morphological evolution is expected to reflect the difference in the viscosity of the polymer blends; it is low (high chain mobility) for the blend with *L*-PF12TBT and high (low chain mobility) for *H*-PF12TBT.

First, we focus on the temperature dependence of the photoluminescence quenching efficiency of PF12TBT (Φ_q)

Table 2. Best PCE and Device Parameters of P3HT/PF12TBT Solar Cells Measured under AM 1.5G Simulated Solar Light Irradiation (intensity: 100 mW cm^{-2})

acceptor	J_{SC} (mA cm^{-2})	FF	V_{OC} (V)	PCE (%)[a]	annealing temperature (°C)[b]
L–PF12TBT	3.80	0.41	1.22	1.90	100
M–PF12TBT	3.30	0.50	1.24	2.04	120
H–PF12TBT	3.88	0.55	1.26	2.70	140

[a]At least five devices were fabricated. The average values were 1.85% for *L*-PF12TBT, 1.93% for *M*-PF12TBT, and 2.61% for *H*-PF12TBT. [b]The annealing temperature corresponding to the highest PCE for each device.

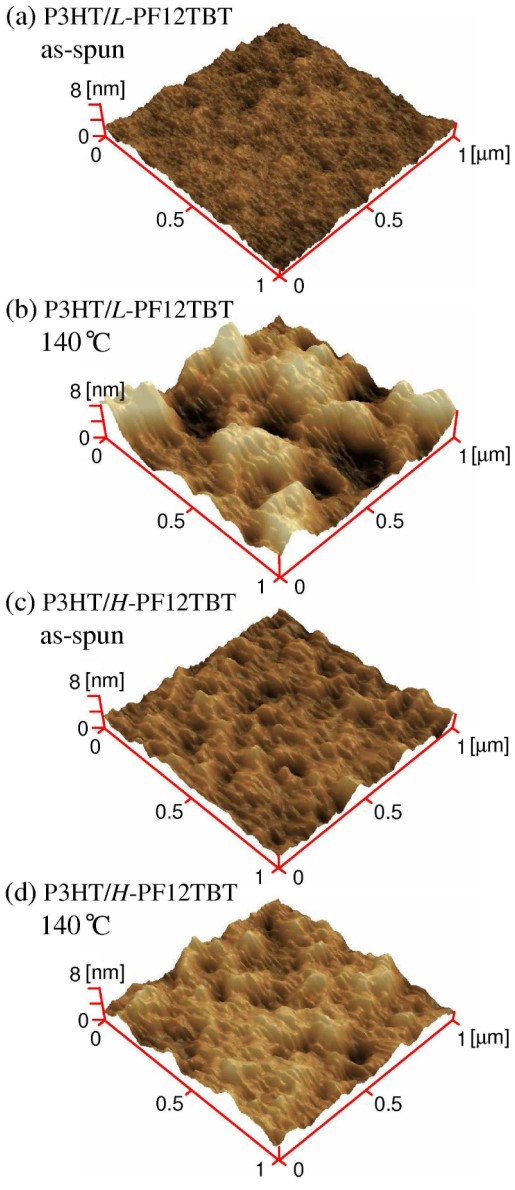

Figure 2. Tapping-mode AFM topographic images (1 μm × 1 μm) of (a, b) P3HT/*L*-PF12TBT and (c, d) P3HT/*H*-PF12TBT blend films spin-coated from chloroform solutions of P3HT and PF12TBT (1:1 weight ratio) on glass substrates: (a, c) as-spun films; (b, d) annealed films at 140 °C for 10 min.

dx.doi.org/10.1021/am300623f | ACS Appl. Mater. Interfaces 2012, 4, 3325–3329

and J_{SC} to discuss the nanoscale phase-separated morphology of PF12TBT in the blends. Before thermal annealing, as shown in Figure 3a, the Φ_q values were in the range 80−90%, regardless

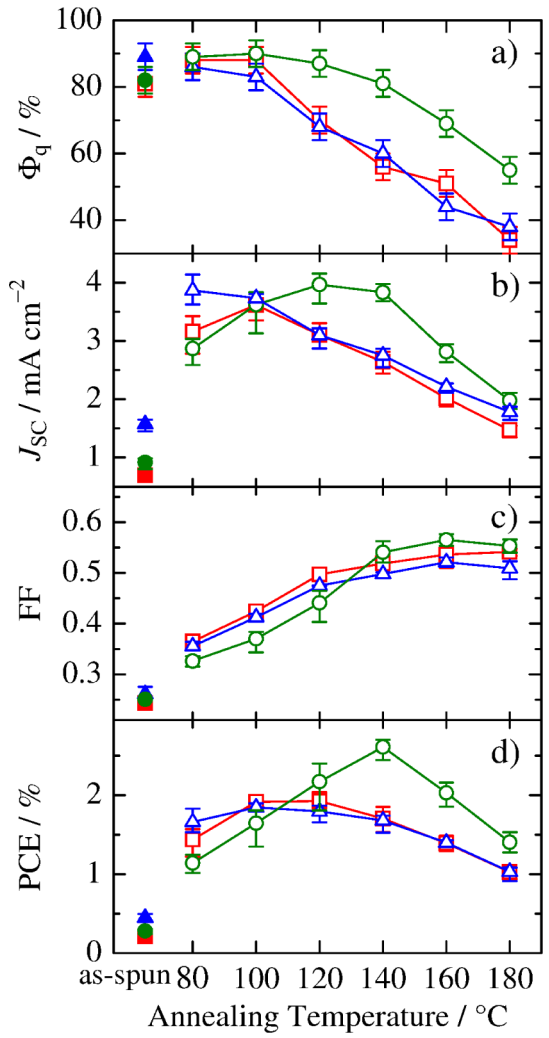

Figure 3. Dependence of Φ_q and device parameters of the P3HT/*L*-PF12TBT (open triangles), P3HT/*M*-PF12TBT (open squares), and P3HT/*H*-PF12TBT (open circles) devices on the annealing temperature under AM 1.5G illumination from a calibrated solar simulator with an intensity of 100 mW cm^{-2}. The closed symbols represent Φ_q and the device parameters for the as-spun devices. All devices were fabricated by spin-coating from a chloroform solution of P3HT and PF12TBT (1:1 weight ratio) and annealed for 10 min.

of M_w, suggesting that all the as-spun blends had well-mixed structures on a nanometer scale. After thermal annealing, Φ_q decreased above a certain annealing temperature that depended on M_w: 80 °C for P3HT/*L*-PF12TBT, 100 °C for P3HT/*M*-PF12TBT, and 120 °C for P3HT/*H*-PF12TBT. On the other hand, as shown in Figure 3b, the maximun J_{SC} was obtained at 80 °C for P3HT/*L*-PF12TBT, 100 °C for P3HT/*M*-PF12TBT, and 120 °C for P3HT/*H*-PF12TBT. In other words, J_{SC} increased at the annealing temperatures at which Φ_q was constant and it decreased over the temperature range where Φ_q decreased. As discussed in our previous report,[11] the Φ_q value provides information about the purity and size of the PF12TBT-rich domains. The high Φ_q (close to 90%) in the case of the P3HT/PF12TBT blends spin-coated from chloroform was related to nanometer-size PF12TBT domains with P3HT as the minor constituent.[11] Thermal annealing should increase the domain purity or domain size. An increase in the domain purity results in an increase in J_{SC} because of the suppression of undesirable exciton quenching inside the domain. On the other hand, an increase in the domain size causes a decrease in the area of the domain interface necessary for charge generation. Thus, the Φ_q value, which remained constant at 90% during the annealing, indicates that the domain size had a length scale smaller than that of exciton diffusion (about 10 nm), although purification proceeded in the domains. The subsequent decrease in Φ_q at higher annealing temperatures suggests an increase in the domain size. Therefore, Φ_q in Figure 3a shows that domain bloating was effectively suppressed in P3HT/*H*-PF12TBT until the blend was annealed at 140 °C, but it was accelerated in P3HT/*L*-PF12TBT even at low annealing temperatures. The slow domain bloating in P3HT/*H*-PF12TBT can be explained in terms of the high glass transition temperature of *H*-PF12TBT (T_g = 90 °C, Table 1) and the reduced chain mobility of high-molecular-weight PF12TBT chains above T_g.[5,23] We conclude that the rate of phase separation can be controlled by varying the M_w value of PF12TBT.

We next focus on the FF to discuss the molecular-weight dependence of the morphological evolution necessary for charge transport. As shown in Figure 3c, the FF increased from 0.25 for as-spun devices to 0.5−0.6 for the devices annealed at 160 °C, and it saturated at higher temperatures. The increase in the FF with temperature can be explained in terms of the purification of PF12TBT-rich domains and the formation of interconnected networks of the domains, because these factors contribute to efficient electron transport. For the P3HT/*L*-PF12TBT device, the FF increased with temperature because of the increase in the domain size. In contrast, for the P3HT/*H*-PF12TBT device annealed at high temperatures, the FF was as high as 0.5−0.6, although the large Φ_q is indicative of well-mixed blend morphology. This finding suggests that the annealing of blends with high-molecular-weight PF12TBT is likely to result in the formation of interconnected networks without increasing the domain size. In addition to the PF12TBT morphology, the P3HT morphology should be considered in order to account for the increase in the FF with temperature. In blends consisting of P3HT and the fluorene-based copolymer poly[2,7-(9,9-dioctylfluorene)-*alt*-5,5-(4′,7′-bis(4-hexyl-2-thienyl)-2′,1′,3′-benzothiadiazole)] (F8TBT), the hole mobility increased by nearly two orders of magnitude upon annealing at 180 °C, because of the ordering of the P3HT chains.[20,24] Indeed, the ordering of P3HT chains by annealing was found in this P3HT/PF12TBT blend from transient ground-state bleaching (GSB) that were analyzed by transient absorption (TA) measurements. The TA measurements were performed for the as-spun and annealed P3HT/*H*-PF12TBT films at temperatures of 100, 120, and 140 °C. In Figure 4, transient GSB (a negative change in the optical density ΔOD) bands are observed at 3 ns, suggesting that holes and electrons were generated on P3HT and PF12TBT, respectively, because singlet excitons of both polymers had already decayed at 3 ns. The charge-induced GSB spectrum of the film annealed at 140 °C showed the most pronounced bleaching peaks at 550 and 600 nm, which are ascribed to the π-stacked P3HT chains.[25−27] The improved π-stacking in the P3HT-rich phase should contribute to efficient hole transport[28] and thus to an increase in the FF. We therefore conclude that both electron transport and hole transport are improved in P3HT/*H*-PF12TBT as a

dx.doi.org/10.1021/am300623f | ACS Appl. Mater. Interfaces 2012, 4, 3325−3329

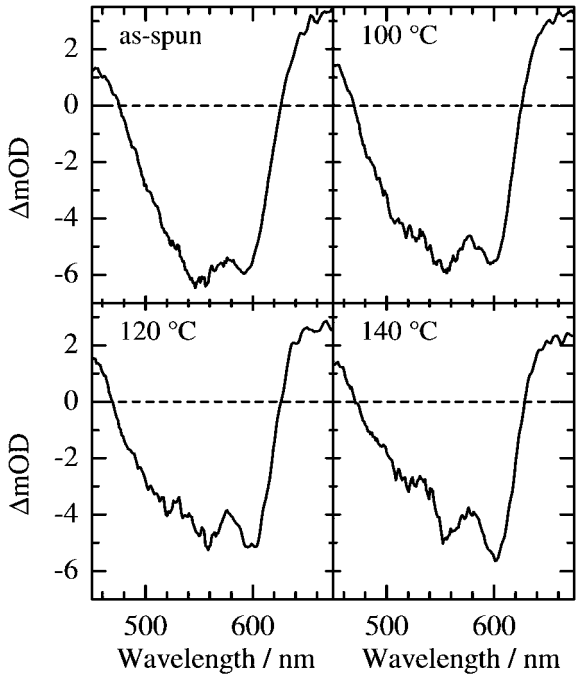

Figure 4. TA spectra for as-spun and annealed P3HT/*H*-PF12TBT blend films measured 3 ns after 400 nm photoexcitation with a 100 fs pulsed laser. The excitation fluence was 45 μJ cm^{-2} (9.1 × 10^{13} photons cm^{-2}) for all measurements.

result of the excellent interconnectivity and thermal purification of the PF12TBT-rich phase and the ordering of P3HT chains; consequently, an increase in the FF is observed.

We finally explain the molecular-weight dependence of the PCE in terms of the balance between J_{SC} and the FF. When P3HT/*L*-PF12TBT was annealed at 80 °C, the FF was still as low as 0.36; in other words, charge transport was poor because of the incomplete formation of interconnected networks of *L*-PF12TBT domains and the incomplete ordering of P3HT chains, although the maximum value of J_{SC} was achieved as a result of the purification of the *L*-PF12TBT domains. At annealing temperatures above 80 °C, the FF increased but J_{SC} decreased as a result of an increase in the domain size. Consequently, the device performance was determined by the balance between the decrease in J_{SC} and the increase in the FF. Thus, the P3HT/*L*-PF12TBT device showed the best PCE at 100 °C. This was also the case for the high-molecular-weight P3HT/*H*-PF12TBT device. However, efficient charge transport can be achieved through the purification of the interconnected *H*-PF12TBT phase and the ordering of P3HT chains in P3HT-rich domains at high annealing temperatures without drastically increasing the domain size. Due to the slow domain bloating of *H*-PF12TBT, J_{SC} reached the maximum value at 120 °C and remained almost unchanged even at 140 °C. We therefore conclude that the highest PCE of 2.7% can be achieved at 140 °C because the FF can be improved to up to 0.55 without decreasing the maximum value of J_{SC}.

In conclusion, the molecular-weight dependence of the PCE is attributed to the difference in the rate of phase separation during annealing. In the blend containing *H*-PF12TBT, the domain size of phase separation has a length scale comparable to that of exciton diffusion even at high annealing temperatures owing to the reduced diffusional mobility of the *H*-PF12TBT chains; such a domain size is necessary for efficient charge generation. Further, a blend morphology consisting of interconnected networks of pure *H*-PF12TBT domains and ordered P3HT chains, which is necessary for efficient charge transport, can be achieved by annealing. This blend morphology is responsible for the PCE of 2.7%, which is the highest ever reported for an all-polymer solar cell.

EXPERIMENTAL SECTION

Materials. PF12TBT samples with three different molecular weights were synthesized and characterized at Sumitomo Chemical Co., Ltd. The weight-average molecular weight M_w, polydispersity index (PDI, given by M_w/M_n, where M_n is the number-average molecular weight), and glass transition temperature T_g of each PF12TBT sample were as follows: *L*-PF12TBT, M_w = 8500 g mol^{-1}, PDI = 1.7, and T_g = 60 °C; *M*-PF12TBT, M_w = 20 000 g mol^{-1}, PDI = 2.0, and T_g = 76 °C; *H*-PF12TBT, M_w = 78 000 g mol^{-1}, PDI = 2.8, and T_g = 90 °C. P3HT was purchased from Aldrich Chemical Co. (Lot MKBD3325). The head-to-tail regioregularity, M_w, and PDI provided on the Certificate of Analysis were 90.0%, 42 300 g mol^{-1}, and 1.9, respectively.[29]

Device Fabrication and Measurements. Indium−tin-oxide (ITO)-coated glass substrates (10 Ω per square) were washed by ultrasonication in toluene, acetone, and ethanol for 15 min each in this order and then dried with N_2 flow. The washed substrates were further treated with a UV−O_3 cleaner (Nippon Laser & Electronics Lab., NL-UV253S) for 30 min. A thin layer (~40 nm) of poly(3,4-ethylenedioxythiophene):poly(4-styrenesulfonate) (PEDOT:PSS, H.C. Stark PH-500) was spin-coated onto the ITO substrate at a spin rate of 3000 rpm for 99 s and dried at 140 °C for 10 min in air. A blend layer of P3HT/PF12TBT was spin-coated on the PEDOT:PSS film at 3000 rpm for 60 s from chloroform (CF) solutions. All P3HT/PF12TBT blend films used in this study were spin-coated from CF solutions which were prepared by mixing P3HT and PF12TBT with a weight ratio of 1:1 as follows: three blend solutions were prepared by dissolving P3HT (6 mg) and *L*-PF12TBT (6 mg) in 1 mL of CF, P3HT (6 mg) and *M*-PF12TBT (6 mg) in 1 mL of CF, and P3HT (5.5 mg) and *H*-PF12TBT (5.5 mg) in 1 mL of CF, respectively. Thickness of the P3HT/PF12TBT blend layers was typically 60 nm. The photoactive layer was thermally annealed for 10 min in a N_2-filled glove box, and then, a calcium interlayer (Ca, 15 nm) and an aluminum electrode (Al, 70 nm) were vacuum-deposited. The *J*−*V* characteristics of the devices were measured by using a direct-current voltage and a current source/monitor (Advantest model R6243) under illumination with AM1.5G simulated solar light with 100 mW cm^{-2}. The light intensity was corrected with a calibrated silicon photodiode reference cell (Bunko-Keiki, BS-520). The active area of the device was 0.07 cm^2. Illumination was carried out from the ITO side. All measurements were performed in N_2 atmosphere at room temperature. At least five devices were fabricated to ensure reproducibility of the *J*−*V* characteristics.

AFM Measurements. AFM images were collected in tapping mode (Shimadzu, SPM-9600) using silicon probes with a resonant frequency of ~330 kHz and a force constant of ~42 N m^{-1} (Nanoworld, NCHR).

Photoluminescence Quenching Measurements. The photoluminescence (PL) spectra were measured for a neat PF12TBT film and P3HT/PF12TBT blend films spin-coated on a glass substrate by using a calibrated fluorescence spectrophotometer (Hitachi, F-4500). Excitation was performed at 392 nm to excite a PF12TBT component mainly (excitation fraction of each component was 73% (PF12TBT) and 27% (P3HT)) and at an incident angle of 30° normal to the substrate. Emission was collected normal to the excitation light. The PL quenching efficiency of PF12TBT in the blend film was evaluated from the ratio of the PL intensity for the P3HT/PF12TBT blend films to that for a neat PF12TBT film after each PL intensity was corrected by variations for PF12TBT absorption at 392 nm.

■ ASSOCIATED CONTENT

Supporting Information

Transient absorption method, dark $J-V$ curve (logarithmic scale) of a P3HT/*H*-PF12TBT solar cell with 2.7% PCE, and all the dark and light $J-V$ curves for three different molecular weight of PF12TBT. This material is available free of charge via the Internet at http://pubs.acs.org

■ AUTHOR INFORMATION

Corresponding Author

*Tel.: +81 75 383 2614 (H.B.); +81 75 383 2612 (S.I.). Fax: +81 75 383 2617 (H.B.); +81 75 383 2617 (S.I.). E-mail: benten@photo.polym.kyoto-u.ac.jp (H.B.); sito@photo.polym.kyoto-u.ac.jp (S.I.).

Notes

The authors declare no competing financial interest.

■ ACKNOWLEDGMENTS

This work was supported by a FIRST Program and a Grant-in-Aid for Young Scientists (B) (22750109) from JSPS, a PRESTO program from JST, and a Global COE program from MEXT.

■ REFERENCES

(1) Nelson, J. *Mater. Today* **2011**, *14*, 462−470.
(2) Ohkita, H.; Ito, S. *Polymer* **2011**, *52*, 4397−4417.
(3) Li, G.; Zhu, R.; Yang, Y. *Nat. Photon* **2012**, *6*, 153−161.
(4) Dennler, G.; Scharber, M. C.; Brabec, C. J. *Adv. Mater.* **2009**, *21*, 1323−1338.
(5) Veenstra, S. C.; Loos, J.; Kroon, J. M. *Prog. Photovolt.: Res. Appl.* **2007**, *15*, 727−740.
(6) McNeill, C. R.; Greenham, N. C. *Adv. Mater.* **2009**, *21*, 3840−3850.
(7) Yan, H.; Collins, B. A.; Gann, E.; Wang, C.; Ade, H.; McNeill, C. R. *ACS Nano* **2012**, *6*, 677−688.
(8) He, X.; Gao, F.; Tu, G.; Hasko, D.; Hüttner, S.; Steiner, U.; Greenham, N. C.; Friend, R. H.; Huck, W. T. S. *Nano Lett.* **2010**, *10*, 1302−1307.
(9) Mulherin, R. C.; Jung, S.; Huettner, S.; Johnson, K.; Kohn, P.; Sommer, M.; Allard, S.; Scherf, U.; Greenham, N. C. *Nano Lett.* **2011**, *11*, 4846−4851.
(10) McNeill, C. R.; Westenhoff, S.; Groves, C.; Friend, R. H.; Greenham, N. C. *J. Phys. Chem. C* **2007**, *111*, 19153−19160.
(11) Mori, D.; Benten, H.; Kosaka, J.; Ohkita, H.; Ito, S.; Miyake, K. *ACS Appl. Mater. Interfaces* **2011**, *3*, 2924−2927.
(12) Holcombe, T. W.; Woo, C. H.; Kavulak, D. F. J.; Thompson, B. C.; Fréchet, J. M. J. *J. Am. Chem. Soc.* **2009**, *131*, 14160−14161.
(13) Zhou, E.; Cong, J.; Wei, Q.; Tajima, K.; Yang, C.; Hashimoto, K. *Angew. Chem. Int. Ed.* **2011**, *50*, 2799−2803.
(14) Arias, A. C.; MacKenzie, J. D.; Stevenson, R.; Halls, J. J. M.; Inbasekaran, M.; Woo, E. P.; Richards, D.; Friend, R. H. *Macromolecules* **2001**, *34*, 6005−6013.
(15) Snaith, H. J.; Arias, A. C.; Morteani, A. C.; Silva, C.; Friend, R. H. *Nano Lett.* **2002**, *2*, 1353−1357.
(16) Shikler, R.; Chiesa, M.; Friend, R. H. *Macromolecules* **2006**, *39*, 5393−5399.
(17) McNeill, C. R.; Watts, B.; Thomsen, L.; Belcher, W. J.; Greenham, N. C.; Dastoor, P. C.; Ade, H. *Macromolecules* **2009**, *42*, 3347−3352.
(18) Swaraj, S.; Wang, C.; Yan, H.; Watts, B.; Lüning, J.; McNeill, C. R.; Ade, H. *Nano Lett.* **2010**, *10*, 2863−2869.
(19) Moore, J. R.; Albert-Seifried, S.; Rao, A.; Massip, S.; Watts, B.; Morgan, D. J.; Friend, R. H.; McNeill, C. R.; Sirringhaus, H. *Adv. Energy Mater.* **2011**, *1*, 230−240.
(20) McNeill, C. R.; Abrusci, A.; Hwang, I.; Ruderer, M. A.; Müller-Buschbaum, P.; Greenham, N. C. *Adv. Funct. Mater.* **2009**, *19*, 3103−3111.
(21) Campbell, A. R.; Hodgkiss, J. M.; Westenhoff, S.; Howard, I. A.; Marsh, R. A.; McNeill, C. R.; Friend, R. H.; Greenham, N. C. *Nano Lett.* **2008**, *8*, 3942−3947.
(22) Schubert, M.; Dolfen, D.; Frisch, J.; Roland, S.; Steyrleuthner, R.; Stiller, B.; Chen, Z.; Scherf, U.; Koch, N.; Facchetti, A.; Neher, D. *Adv. Energy Mater.* **2012**, *2*, 369−380.
(23) Sperling, L. H. In *Introduction to Physical Polymer Science*, 4th ed.; Wiley-Interscience: Hoboken, NJ, 2006.
(24) Flesch, H. G.; Resel, R.; McNeill, C. R. *Org. Electron.* **2009**, *10*, 1549−1555.
(25) Brown, P. J.; Sirringhaus, H.; Harrison, M.; Shkunov, M.; Friend, R. H. *Phys. Rev. B* **2001**, *63*, 125204.
(26) Clark, J.; Silva, C.; Friend, R. H.; Spano, F. C. *Phys. Rev. Lett.* **2007**, *98*, 206406.
(27) Guo, J.; Ohkita, H.; Benten, H.; Ito, S. *J. Am. Chem. Soc.* **2009**, *131*, 16869−16880.
(28) Chang, J. F.; Clark, J.; Zhao, N.; Sirringhaus, H.; Breiby, D. W.; Andreasen, J. W.; Nielsen, M. M.; Giles, M.; Heeney, M.; McCulloch, I. *Phys. Rev. B* **2006**, *74*, 115318.
(29) The P3HT samples employed both in the previous paper (ref 11) and in the present study are purchased from Aldrich Chemical Co.: the catalogue number is the same, which was labeled with a typical molecular weight of M_w = 87 000 g mol^{-1}, but the batch number is different. We have measured the molecular weight of both P3HT for different batch numbers and confirmed that both are similar to each other.